RESEARCH ARTICLE
doi: 10.2306/scienceasia1513-1874.2007.33.175

ScienceAsia 33 (2007): **175-185**

Behavior of Reinforced Concrete Bridge Pier Columns Subjected to Moderate Seismic Load

Sumnieng Ongsupankul[a*], Torkul Kanchanalai[b] and Kazuhiko Kawashima[c]

[a] Department of Civil Engineering, South-East Asia University, Bangkok, Thailand.
[b] Department of Civil Engineering, Kasetsart University, Bangkok, Thailand.
[c] Department of Civil Engineering, Tokyo Institute of Technology, Tokyo, Japan.

* Corresponding author, E-mail: sumnieng@sau.ac.th

Received 25 Jan 2006
Accepted 27 Sep 2006

ABSTRACT: This paper presents the results of the test of six reinforced concrete bridge column specimens and of six analytical specimens subjected to constant axial load and cyclic lateral load. The objective of the investigation is to report the strength and ultimate displacement of the square columns having different amount and arrangement of tie bars. Fiber element inelastic analyses were conducted to verify the test results and were in reasonable agreement with the experimental study results. It was found that the criterion of limiting lateral strain in the concrete core gave satisfactory estimate of the maximum column deflection. Further analytical study of six columns with different tie reinforcement ratio and subjected to varying cyclic loads was performed. Based on the experimental and analytical studies of reinforced concrete columns subjected to the axial loads ranging between $0.05f_cA_g$ and $0.12f_cA_g$, tie reinforcement ratio, $\rho_s = 0.50\%$ which corresponds to approximately 60% of the minimum amount required by the AASHTO seismic provision exhibits moderate ductility ratio being 4.3 and 7.3 for axial loads of $0.12f_cA_g$ and $0.05f_cA_g$ respectively.

KEYWORDS: Bridge pier, Seismic design, Reinforced concrete column, Ductility, Strength.

INTRODUCTION

As for seismic hazard map [1], northern and western regions of Thailand are located in moderate seismicity of zones 2 and 3 based on AASHTO [2] specification where the peak ground acceleration (PGA) is in the range 0.15g to 0.25g. Typical highway bridges have two column piers supporting prestressed girders. In the past, bridges in high seismicity region were severely damaged from seismic hazards. Although Thailand is not prone to strong earthquakes, the needs for proper seismic study for highway bridges are to be emphasized.

This research investigated the behavior of typical reinforced concrete bridge piers of six 400 mm × 400 mm square columns. The columns were subjected to constant axial load and cyclic lateral load. The tests were conducted at Kawashima laboratory of department of civil engineering, Tokyo institute of technology. The fiber element inelastic analyses were conducted and compared with the experiment results.

Test Specimens

Test specimens were constructed by scaling down full size bridge columns having 600 mm × 600 mm and 800 mm × 800 mm cross sections. All specimens had the same dimension of 400 mm × 400 mm and effective height of 1550 mm. The specimen D1 was scaled down from 800 mm × 800 mm full size columns. Other specimens were scaled down from 600 mm × 600 mm full size members. The longitudinal reinforcement consisted of 13 mm diameter deform bars with yield strength of 390 MPa. Tie reinforcement is of 6 mm diameter round bars with yield strength of 245 MPa and having 135 degree hooks with development length of 75 mm. The concrete strength is in the range from 29.61 to 32.36 MPa. The amount of lateral reinforcement was varied to investigate its confining effect on strength and ductility of the specimens. Strain gages were attached to the longitudinal bars and tie bars in the column base region. The details of the cross section reinforcement and the column model are shown in Fig.1 and Fig. 2 and the details of column characteristic are summarized in Table 1.

Tie reinforcement ratios, ρ_s: (A_{sh}/sh_c), of specimens A1, A2, B1 and B2 were designed corresponding to 25% of the minimum total cross-section area of rectangular hoops and crossties based on AASHTO [2] with seismic performance for zone 3 ($0.19g < a < 0.29g$) and zone 4 ($a > 0.29g$), being the larger of Eq. (1) and (2). Cross-tie stirrups were provided in specimen B1 and B2. The tie reinforcement ratio of specimen D1 was designed corresponding to the minimum hoops based on AASHTO [2] with non-seismic performance and specimen C1 was designed based on AASHTO [2] with non-seismic performance and having larger spacing of tie bars than that of specimen D1 and without the cross ties.

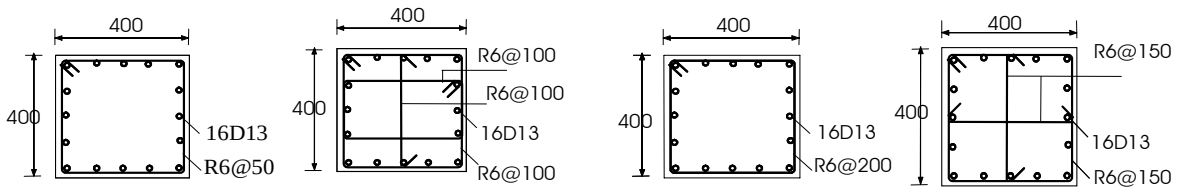

Fig 1. Cross-section of columns.

$$A_{sh} = 0.12 s h_c \frac{f_c'}{f_{yh}} \quad (1)$$

$$A_{sh} = 0.3 s h_c \frac{f_c'}{f_{yh}} \left(\frac{A_g}{A_c} - 1 \right) \quad (2)$$

where

A_{sh} = cross section area of confinement reinforcement.

s = spacing of transverse reinforcement along the axis of the member; s < 10 cm = 1/4 of the minimum member dimension, whichever is smaller.

h_c = cross-sectional dimension of column core measured out-to-out of transverse reinforcement.

A_g = gross area of section.

A_c = core section area of a structural member measured out-to-out of transverse reinforcement.

f_c = specified concrete strength.

f_{yh} = specified yield strength of transverse reinforcement.

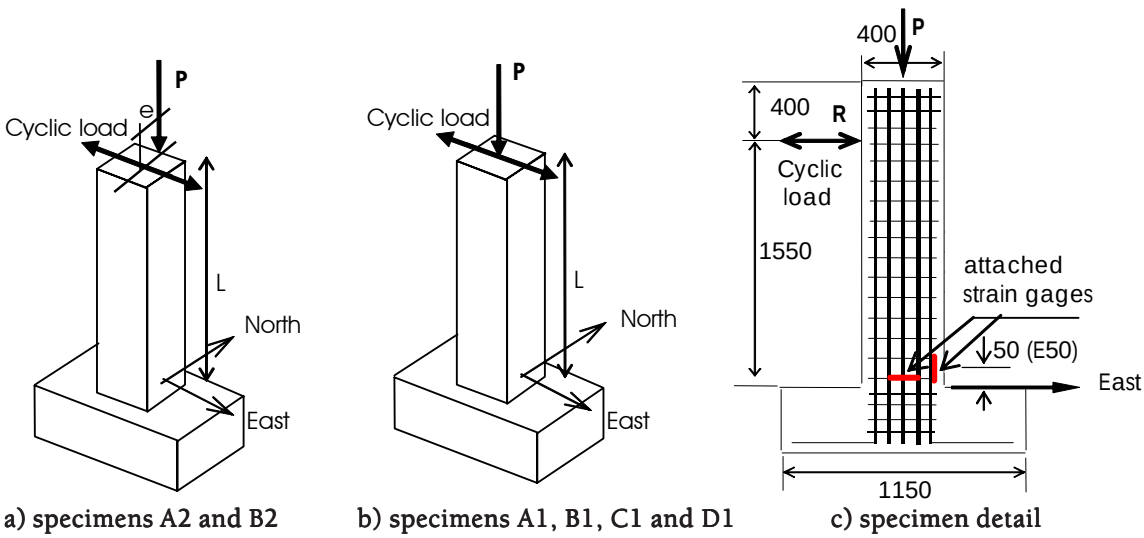

Fig 2. Column model.

Table 1. Detailing of column specimens.

Specimens	A1	A2	B1	B2	C1	D1
Section size, $b \times h$ (mm)	400 × 400 (Square)					
Effective height, L (mm)	1550					
Effective depth, d (mm)	360					
Ratio of tie reinforcement {$(A_{sh}/(sh_c)$, ρ_s (%)}	0.37		0.37		0.09	0.19
Volume ratio of tie bar {(V_{core}/V_{sh}), ρ_{st},(%)}	0.75		0.93		0.19	0.50
Cylinder strength of concrete (f_c') (MPa)	32.36		29.61		32.36	29.61
Longitudinal reinforcement (%) (F_y =390 MPa)	1.27% (16D13 SD345)					
Tie reinforcement (F_y = 245 MPa)	1-R6@50		2-R6@100		1-R6@200	1.5-R6@150
Axial force (kN)	384 kN					
Axial force index {$P/(f_c' A_g)$}	0.074		0.081		0.074	0.081
Eccentricity (e/h)	0	0.15	0	0.15	0	0

Loading

Each specimen was subjected to the constant axial load of 384 kN applied by a vertical actuator (MTS Model l243) and the cyclic lateral load was applied by a horizontal actuator (MTS Model 244) in east (E) and west (W) direction. The cyclic loading history as shown in Fig. 3 was controlled by applying the lateral load to produce a step-wise displacement starting from 0.5% drift ratio and increasing the cycle of displacement with an increment of 0.5% drift ratio in 30 seconds in each step until final failure was observed.

The effect of eccentricity of vertical loading was considered. The specimens A1, B1, C1 and D1 were loaded by concentric loading and the specimens A2 and B2 were loaded by eccentric loading with the eccentricity of 0.15 time of column depth. The provision of eccentricity is to simulate the effect of the offset of traffic truck load in the transverse direction. The strain gages were attached to longitudinal bars and tie bars in the column base region to monitor the steel strain during the tests. The general test set-up was shown in Fig. 4.

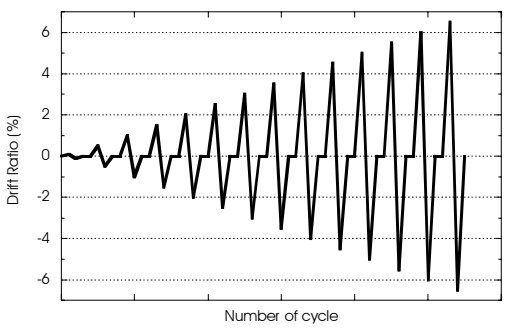

Fig 3. Relative cyclic load histories.

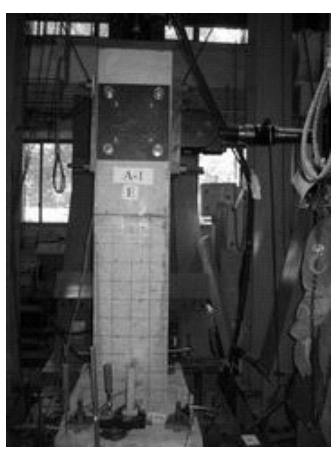

Fig 4. Test setup.

Test Results

Specimen A-1 was subjected to an axial load index, $P/f_c'A_g = 0.074$ applied concentrically and to cyclic lateral displacement loading. After flexural cracks appeared, the measured vertical reinforcement strain reached the yield strain, 0.002 at 0.76% drift ratio while the average measured lateral load, (R) being 124.49 kN and lateral displacement, (Δ_y) being 11.75 mm. The hysteresis behavior under the displacement loading reached the maximum strength of 151.76 kN. When the drift ratio was 3%, the concrete cover started to spall off on the compression side and intensive spalling of concrete occurred at the bottom at 4.5% drift ratio. When the drift ratio was 5.5%, the vertical bars on the east side were buckled and tie bars were exposed outward completely. The measured strain in the tie bars on north side and east side were reached yielded level at 3% and 5% drift ratios respectively. The vertical bars were buckled and tie bars were exposed completely on the west side at 6% drift ratio. Finally, when the specimen was pushed to 6.5% drift ratio, the core concrete was crushed and vertical bars were buckled totally. The severely damaged zone was 30 cm from the base.

Specimen A-2 was subjected to an axial load index, $P/f_c'A_g = 0.074$ applied eccentrically at $0.15h$ in the transverse direction and to cyclic lateral displacement loading. After flexural cracks appeared, the measured vertical reinforcement strain reached the yield strain, at 0.79% drift ratio while the average measured lateral load, (R) being 121.13 kN and lateral displacement, (Δ_y) being 12.19 mm. The hysteresis behavior under the displacement loading reached the maximum strength of 141.11 kN. When the drift ratio was 3%, the concrete cover started to spall off on the compression side and intensive spalling of concrete occurred at the bottom at 4.5% drift ratio. When the drift ratio was 5.5%, the vertical bars on the east side were buckled and tie bars were exposed outward. The measured strain in the tie bars on north side and east side reaches yielded level at 4.5% and 5.5% drift ratio respectively. The vertical bars were buckled and ties bars were exposed completely on the west side at 6% drift ratio. Finally, when the specimen was pushed to 6.5% drift ratio, the core concrete was crushed and vertical bars were buckled totally. The severely damaged zone was 31 cm from the base.

Specimen B-1 was subjected to an axial load index $P/f_c'A_g = 0.081$ applied concentrically and to cyclic lateral displacement loading. After flexural cracks appeared, the measured vertical reinforcement strain reached the yield strain, at 0.67% drift ratio while the average measured lateral load, (R) being 121.17 kN and lateral displacement, (Δ_y) being 10.40 mm. The hysteresis behavior under the displacement loading reached the maximum strength of 154.1 kN. When the drift ratio

was 3.5%, the concrete cover started to spall off on the compression side and intensive spalling of concrete occurred at the bottom at 4% drift ratio. When the drift ratio was 4.5%, the vertical bars on the corner of east and west sides were buckled and tie bars were exposed outward. The measured strain in the outer loop tie bars on north side and east side reached yielded level at 5% drift ratio while the measured strain in the inner loop tie bars on north side reached yielded level at 5.5% drift ratio. The severely damaged zone was 26 cm from the base.

Specimen B-2 was subjected to an axial load index of $0.081 f_c A_g$ applied eccentrically and to cyclic lateral displacement loading. After flexural cracks appeared, the measured vertical reinforcement strain reached the yield strain, at 0.69% drift ratio while the average measured lateral load, (R) being 113.1 kN and lateral displacement, (Δ_y) being 10.66 mm. The hysteresis behavior under the displacement loading reached the maximum strength of 141.23 kN. When the drift ratio was 4%, the cover concrete surface started to spall off on the compression side and intensive spalling of concrete occurred at the bottom at 4.5% drift ratio. At 5% drift ratio, the vertical bars on all corners were buckled and tie bars were exposed outward. The measured strain in the outer loop tie bars on north side and east side reached yielded level at 5% and 5.5% drift ratios respectively. The severely damaged zone was 28 cm from the base.

Specimen C-1 was subjected to an axial load index of $P/f_c A_g = 0.074$ applied concentrically and to cyclic lateral displacement loading. After flexural cracks appeared, the measured vertical reinforcement strain reached the yield strain, at 0.76% drift ratio while the average measured lateral load, (R) being 132.41 kN and lateral displacement, (Δ_y) being 13.51 mm. The hysteresis behavior under the displacement loading reached the maximum strength of 144.52 kN. When the drift ratio was 3%, the concrete cover started to spall off on the compression side. When the drift ratio was 4%, intensive spalling of concrete occurred; vertical bars were buckled and tie bars were exposed outward completely. The measured strain in the tie bars on north side and east side reached yielded level at 3% and 5% drift ratios respectively. At 4.5% drift ratio, the vertical bars at all corners buckled and ties bar were exposed outward. Then all vertical bars buckled completely when drift ratio reached 5%. Finally, when the specimen was pushed to 5.5% drift ratio, the diagonal shear cracks appeared and vertical bars were buckled totally. The severely damaged zone was 43 cm from the base.

Specimen D-1 was subjected to an axial load index of $P/f_c A_g = 0.081$ applied concentrically and to cyclic lateral displacement loading. After flexural cracks appeared, the measured vertical reinforcement strain reached the yield strain at 0.71% drift ratio while the average measured lateral load, (R) being 126.95 kN and lateral displacement, (Δ_y) being 11.04 mm. The hysteresis behavior under the displacement loading reached the maximum strength of 147.16 kN. When the drift ratio was 3%, the concrete cover started to spall off on the compression side and intensive spalling of concrete occurred at the bottom at 3.5% drift ratio. When the drift ratio was 4%, the vertical bars on the corners were buckled and tie bars were exposed outward. The measured strain in the tie bars on north side and east side reached yielded level at 2% and 5% drift ratios respectively. Vertical bars were buckled on the east side at 4.5% drift ratio and all vertical bars were buckled and ties were exposed extensively at 5% drift ratio. Finally, when the specimen was pushed to 5.5% drift ratio, the core concrete was crushed. The severely damaged zone was 35 cm from the base.

The measured steel strain in the strain gages in the specimens A1 and D1 attached to the first hoop were shown in Fig. 5. The gages E37 and E50 were 37 and 50 mm respectively from the footing top. The results of lateral cyclic load vs. hysteresis displacement relationship and failure development of the specimens are shown in Fig. 6 and Fig. 7 respectively.

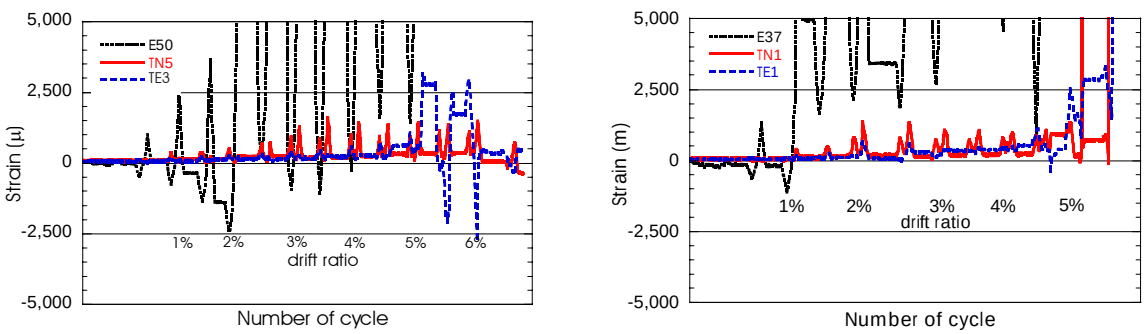

a) specimen A1 b) specimen D1

Fig 5. Measured strain in reinforcement in specimens A1 and D1.

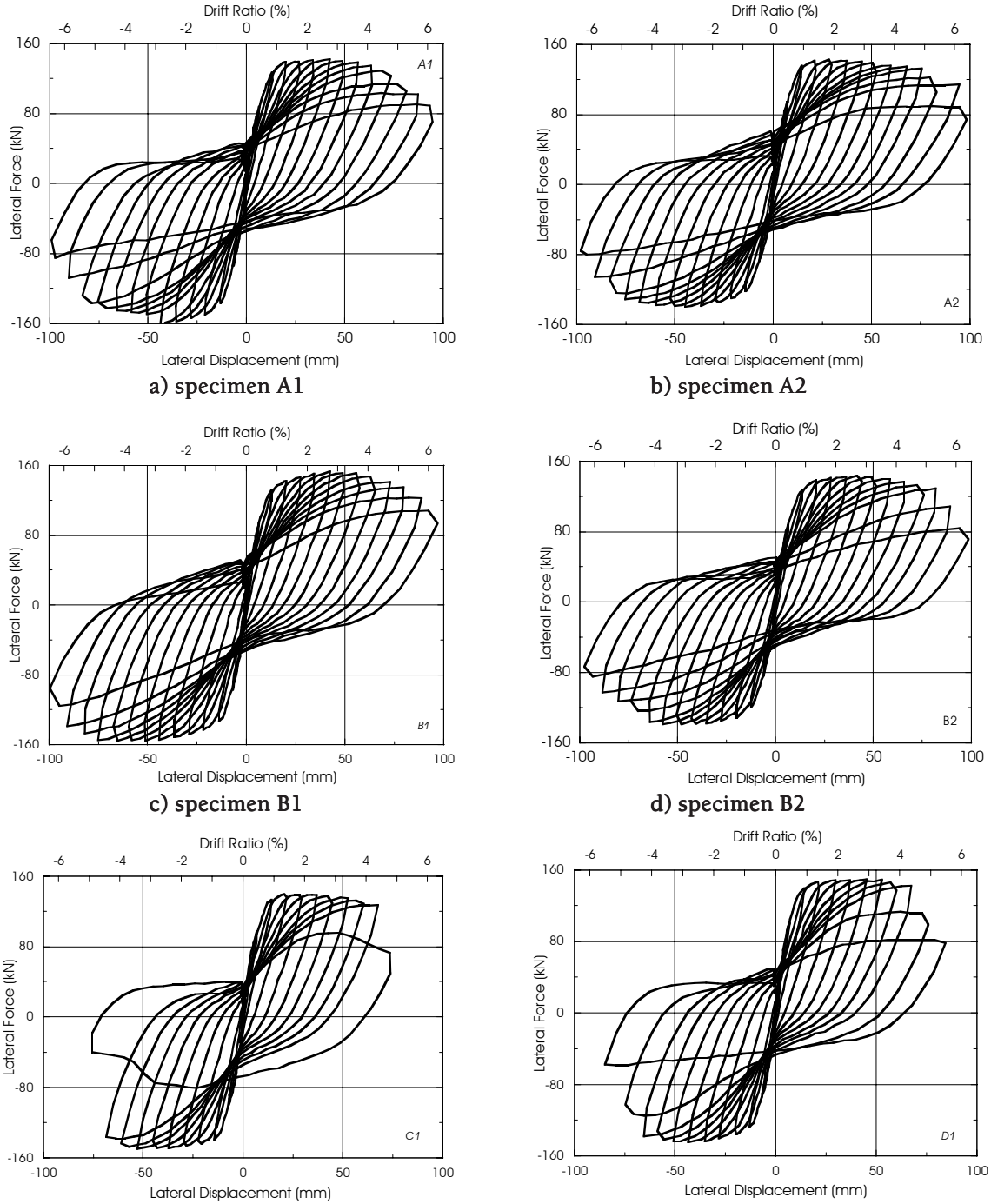

a) specimen A1 b) specimen A2

c) specimen B1 d) specimen B2

e) specimen C1 f) specimen D1

Fig 6. Lateral forces vs. lateral displacement.

The dissipation energy (ΔW_i) in one loop of hysteresis displacement is determined by integrating the area bounded by the hysteresis loop as indicated by Eq. (3). The accumulated dissipation energy (ΔW) in the column specimens is determined by Eq. (4).

$$\Delta W_i = \int_{-u_{min}}^{u_{max}} (F_l(u) - F_{ul}(u))du \quad (3)$$

$$\Delta W = \sum_i \Delta W_i \quad (4)$$

where $F_l(u)$ and $F_{ul}(u)$ are the forces at displacement, u during loading and unloading process.

Fig. 8 shows the dissipation energy vs. drift ratio of the test specimens. The dissipation energy of specimens A2 and B2 subjected to eccentric axial loads is not

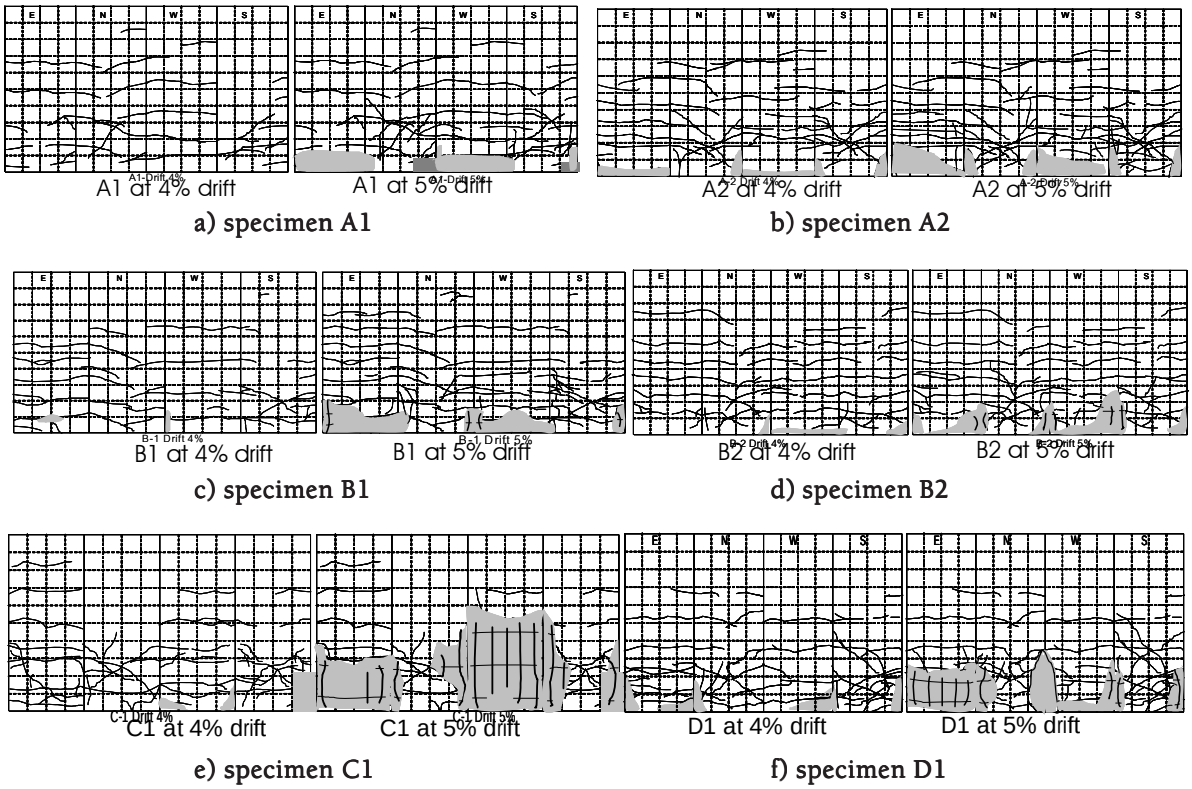

Fig 7. Failure mode of specimens with drift ratio = 4% and 5%.

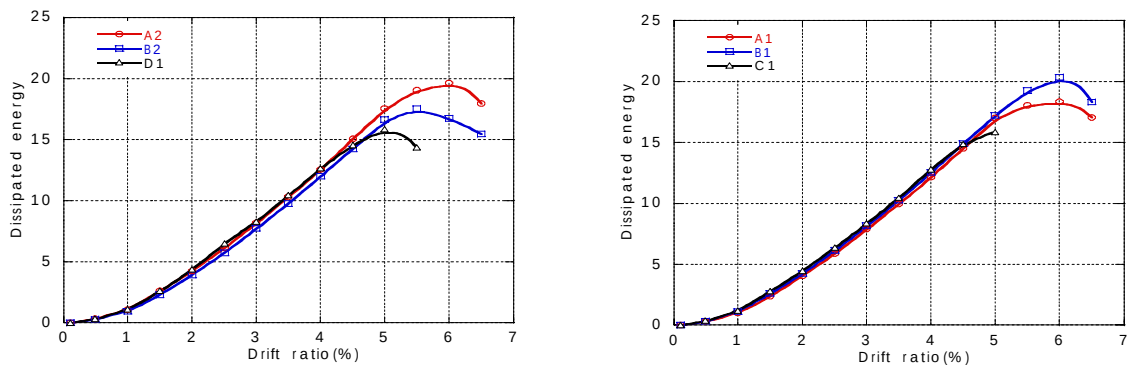

Fig 8. Comparison of Dissipation Energy.

significantly different than the dissipation energy of specimens A1 and B1 when the axial loads were concentric.

The energy is also summarized in Table 2.

Table 2 shows the summary the test results of lateral yield force (R_y), displacement at yield force (Δ_y), maximum lateral force (R_{max}), maximum displacement (Δ_u) and the dissipation energy of the specimens. The maximum displacement (column 5, table 2) was determined when the lateral force was unloaded to 75% of maximum lateral force [3]. The mode of failure at the end of the tests of specimens A1, A2, B1, B2 and D1 is flexural failure while that of specimen C1 being flexural-shear failure.

It can be seen from Table 2 and Fig. 8 that increasing the amount of tie bars does not affect the maximum lateral load force, R_{max} and the yield lateral force, R_y. which increasing the amount of tie bars increases Δ_u and dissipation energy of the specimens. Specimen B1 having cross closed hoop ties tends to attain larger strength, R_{max} and dissipation energy than group A specimens. Fig. 9 shows the failure zone of the specimens. It was observed that cross closed -hoop ties provided in group B specimens are more effective in

Table 2. Compared test results.

Type	Experiment R_y (kN)	Δ_y (mm)	R_{max} (kN)	Δ_u (mm) at 75% of R_{max}	Δ_{u2} (mm)	Accumulate Dissipated Energy (kN-m)	Failure mode	Analytical verification R_y (kN)	Δ_y (mm)	R_{max} (kN)	Δ_u (mm)
A-1	124.49	11.75	151.76	85.07	70.2	128.64	Flexural	105.51	12.56	137.16	37.37
A-2	121.13	12.19	141.11	89.36	51.25	134.75	Flexural	89.7	10.22	137.00	34.88
B-1	121.17	10.40	154.10	92.45	79.5	135.51	Flexural	104.4	12.62	134.75	49.83
B-2	113.10	10.66	141.23	85.78	56.93	123.40	Flexural	86.36	10.05	134.53	31.33
C-1	132.41	13.51	144.52	69.97	46.5	77.64	Flexural-shear	107.62	12.33	137.95	31.75
D-1	126.95	11.04	147.16	73.70	54.25	91.14	Flexural	106.99	12.83	135.34	31.56

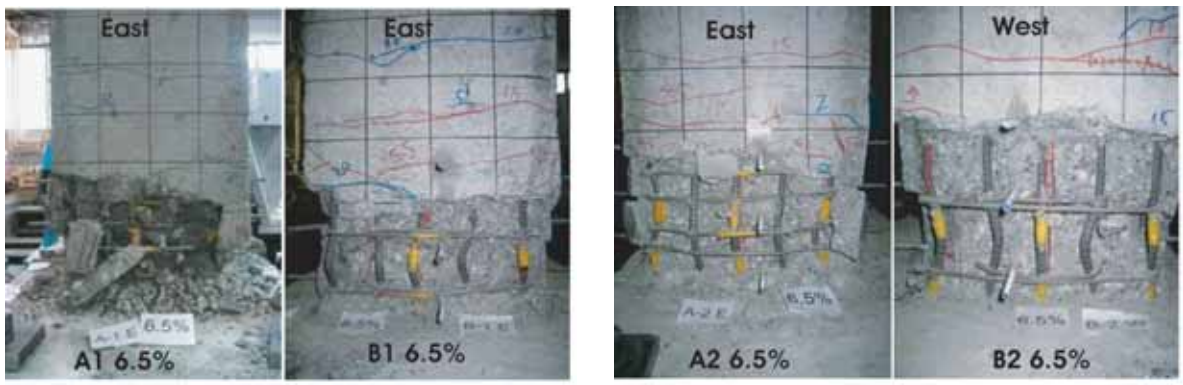

a) specimen A-1 and B1 b) specimen A-2 and B2

Fig 9. Final failure of group A and group B specimens at 6.5% drift.

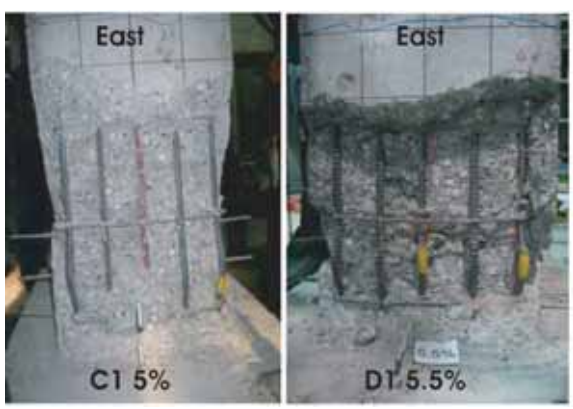

Fig 10. Final failure of specimen C1 at 5% and D1 at 5.5% drift.

reducing outward buckling of the main hoop reinforcement leg and preventing crushing of core concrete than group A specimens. Also the cross ties in specimen D1 are effective in preventing the crushing of core concrete as compared with specimen C1 shown in Fig 10.

Analytical Verification

Hysteresis behavior of the specimens was analyzed by a fiber element model using the TDAP3 program.

Fig. 11 shows the column model being a cantilever column having plastic hinge zone connected to a beam element. The plastic hinge length, (l_p) based on Priestley et al [4] is given by Eq. (5).

$$l_p = 0.08L + 0.022 d_b f_y \quad (5)$$

where

L = length of member between critical section and point of lateral loading (m)

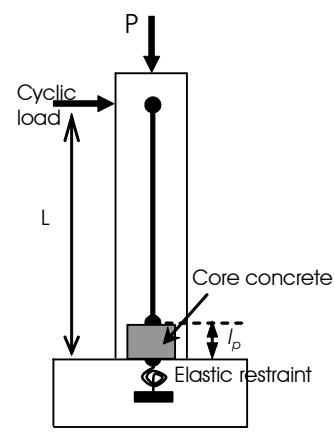

Fig 11. Analytical model.

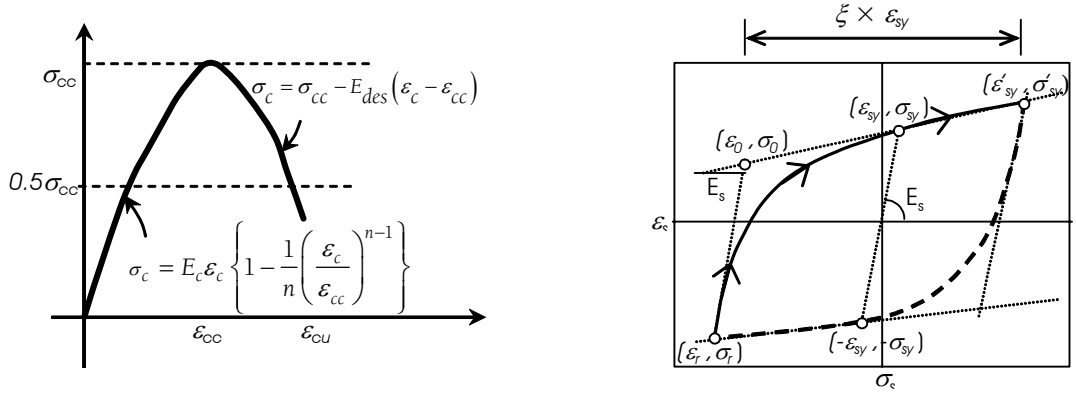

a) confined concrete b) vertical reinforcement

Fig 12. Stress vs. Strain model.

d_b = longitudinal bar diameter (m)
f_y = yield stress of longitudinal bars (MPa)

The plastic hinge length for specimens A1, A2 B1, B2 and D1 is 240 mm and 260 mm for specimen C1. Inelastic materials behavior was used in this analysis. The stress vs. strain model of confined concrete was idealized based on Hoshikuma et al [5] shown in Fig. 12a and was expressed as

$$\sigma_c = E_c\varepsilon_c\left\{1-\frac{1}{n}\left(\frac{\varepsilon_c}{\varepsilon_{cc}}\right)^{n-1}\right\}.....0\le\varepsilon_c\le\varepsilon_{cc} \quad (6)$$

$$= \sigma_{cc} - E_{des}\left(\varepsilon_c-\varepsilon_{cc}\right).....\varepsilon_{cc}\le\varepsilon_c\le\varepsilon_{cu} \quad (7)$$

$$n = \frac{E_c\varepsilon_{cc}}{E_c\varepsilon_{cc}-\sigma_{cc}} \quad (8)$$

$$\sigma_{cc} = \sigma_{ck} + 0.76\rho_s\sigma_{sy} \quad (9)$$

$$\varepsilon_{cc} = 0.002 + 0.0132\frac{\rho_s\sigma_{sy}}{\sigma_{ck}} \quad (10)$$

$$E_{des} = 11.2\frac{\sigma_{ck}^{\ 2}}{\rho_s\sigma_{sy}} \quad (11)$$

Where σ_{cc} and ε_{cc}: are the maximum strength of confined concrete and the strain corresponding to σ_{cc} respectively, E_{des}: stiffness at descending branch, ε_{cu}: ultimate strain, σ_{ck}: concrete strength, σ_{sy}: yield strength of tie bars, ρ_s: volumetric tie bar ratio.

For unconfined concrete, the stress vs. strain model was idealized based on the model by Sakai and Kawashima [6] as shown in Eq. (12) and Eq. (13).

$$\sigma_c = E_c\varepsilon_c\left\{1-\frac{1}{n}\left(\frac{\varepsilon_c}{0.002}\right)^{n-1}\right\}.....0\le\varepsilon_c\le\varepsilon_{cc} \quad (12)$$

$$= \frac{\sigma_{cc}}{0.005}\left(0.007-\varepsilon_c\right)...\varepsilon_{cc}\le\varepsilon_c\le\varepsilon_{cu} \quad (13)$$

The idealized stress vs. strain model of steel reinforcement was based on Menegotto-Pinto model [7] and was also shown in Fig. 12b.

Fig. 13 presents the comparison of the lateral force vs. lateral displacement hysteresis obtained from the analytical and experimental results. The analytical cyclic lateral forces of specimens A1, A2 and B2 were close to those of the experimental results at 1% 1.5% and 2% drift ratios. For specimen B1, the experimental cyclic lateral force is more than analytical result for the drift ratios between 2% to 5%.

The compressive stress versus drift ratio of core concrete in all the specimens was calculated by fiber element method as shown in Fig. 14. When the compressive stress in core concrete on the descending branch was beyond 50% of the core concrete peak stress ($f_{cc}^{'}$), crushing of core concrete and bucking of longitudinal reinforcement occurred. According to Hoshikuma et al [5], the column failure deformation was defined when the stress of core concrete on the descending branch reached 50% of $f_{cc}^{'}$. The analytical results of cyclic lateral force and displacement shown in Table 2 (see column 6 of Table 2). The axial strain at 50% of $f_{cc}^{'}$ was used to observe Δ_u of the specimens in the experiments. For each specimen, the lateral strain in concrete core at failure is the axial strain times the Poisson ratio of 0.2. This is also the strain in the tie bars and the drift ratios can be recorded. It can be observed that the analytical behavior is in reasonable agreement with experimental results.

Further analysis of the behavior of specimens with moderate tie reinforcement was conducted using TDAP program. Table 3 shows the characteristic of the six analytical specimens having tie reinforcement patterns similar to the test specimen D1 and tie reinforcement ratio being in the range of 0.19 % to 0.56 %. The constant axial load was applied and the lateral cyclic load was applied at the top of the columns by increasing the displacements step wisely from 1% drift ratio with an increment of 0.5% drift ratio up to about 5% drift ratio. The number of unloading and reloading was 3

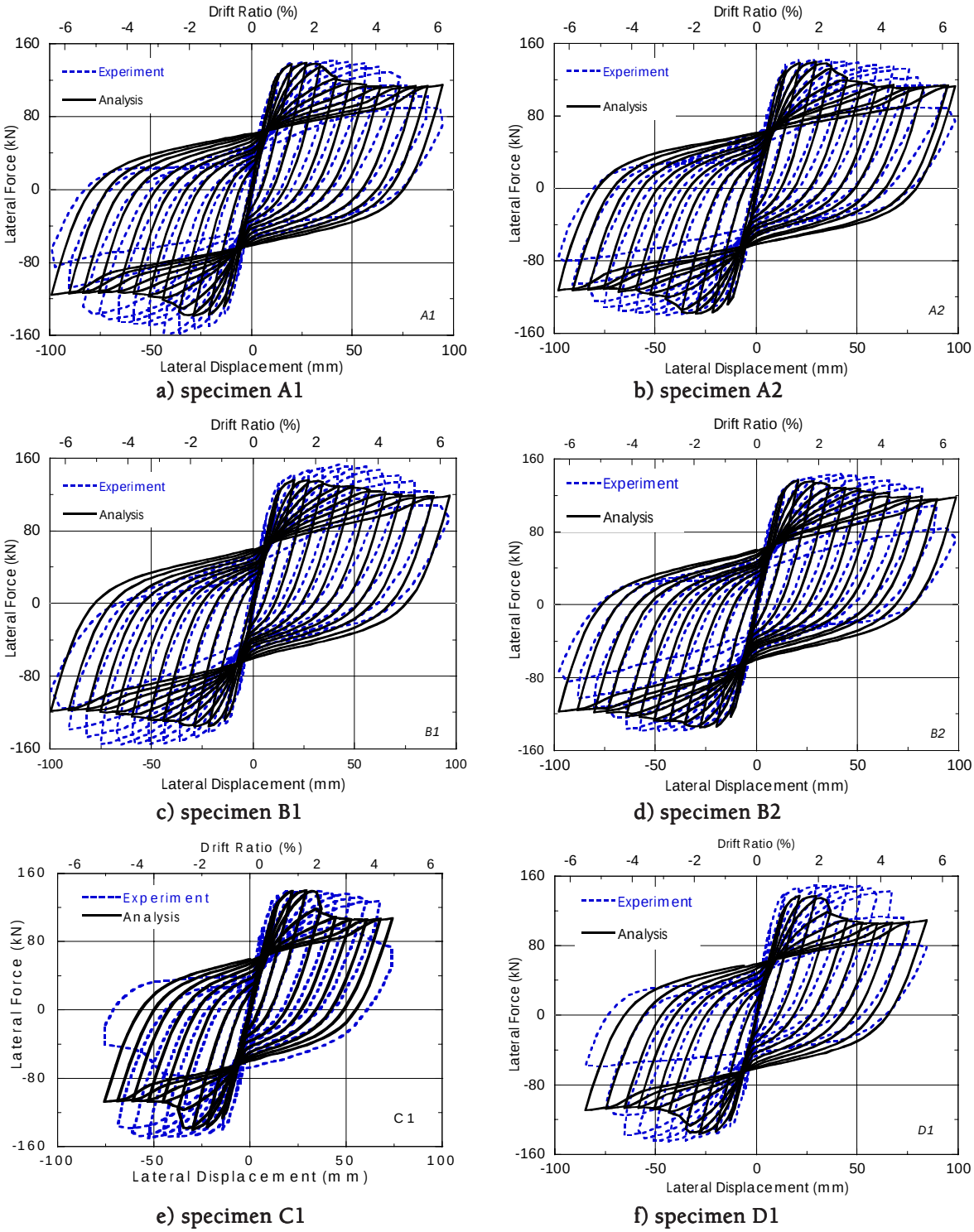

Fig 13. Comparisons of analytical and experimental hysteresis.

cycles for each incremental step.

The analytical results are shown by the envelope curves of the relationship of the compressive stress in the core concrete versus drift ratio for all six specimens in Fig. 15. The first yield loads, maximum loads and the corresponding deflection and drift ratios are summarized in Table 4. Based on Hoshikuma et al [5], the ductility of specimens H1, M1 and L1 are 4.71, 3.61 and 2.64 respectively for the axial force level being $0.12f_cA_g$. For the axial force level being $0.05f_cA_g$, the

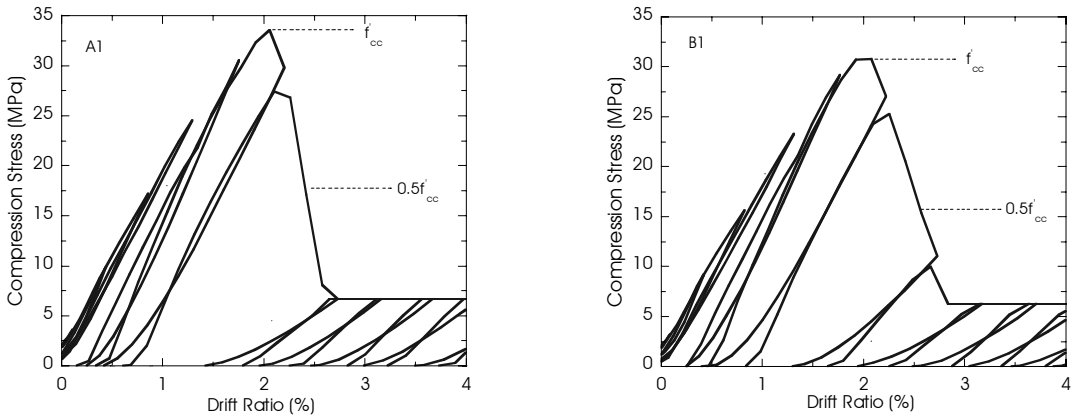

a) specimen A1 b) specimen B1

Fig 14. Compressive stresses in core concrete and drift ratio .

Table 3. Analytical specimens.

Specimens	H1	H0	M1	M0	L1	L0
Section size, $b \times h$ (mm)	400 × 400 (Square)					
Effective height, L (mm)	1400					
Effective depth, d (mm)	360					
Longitudinal reinforcement ratio (%) (F_y =390 MPa)	1.27% (16D13SD40)					
Cylinder strength of concrete (f'_c) (MPa)	28					
Ratio of tie reinforcement {($A_{sh}/(sh_c)$, ρ_s (%)}	0.56		0.37		0.19	
Volume ratio of tie bar {(V_{core}/V_{sh}), ρ_{st},(%)}	1.5		1.0		0.50	
Axial force (kN)	537	224	537	224	537	224
Axial force index {$P/(f'_c A_g)$}	0.12	0.05	0.12	0.05	0.12	0.05
Tie reinforcement (F_y = 390 MPa)	1.5-D6@50mm		1.5-D6@75mm		1.5-D6@150mm	

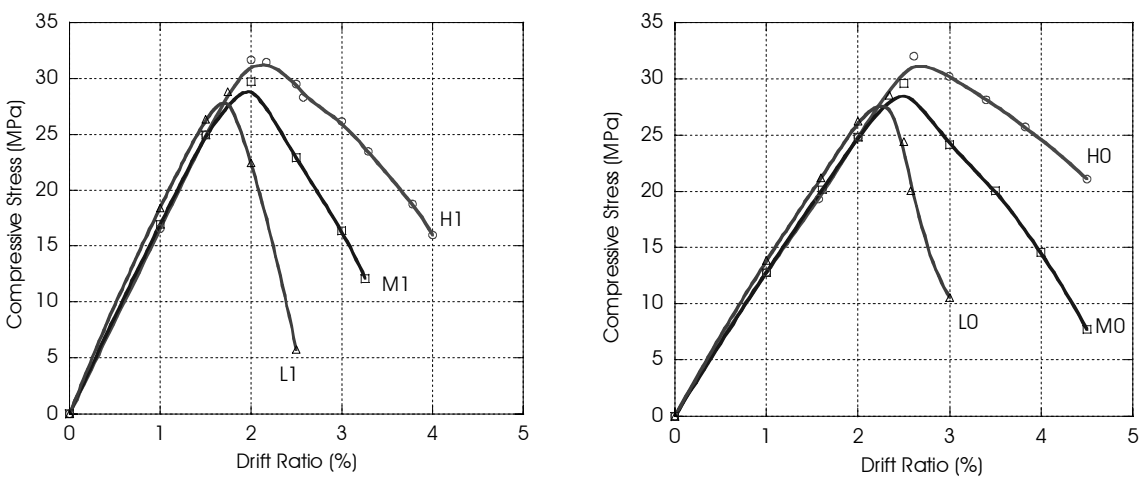

a) axial force (P) = $0.12 f'_c A_g$ b) axial force (P) = $0.05 f'_c A_g$

Fig 15. Compressive stress and drift ratio in core concrete.

ductility of specimens H1, M1 and L1 are 7.84, 5.90 and 4.22 respectively.

The effect of tie reinforcement ratio on the ductility of pier columns for moderate seismicity is shown in Fig. 16 which presents the relationship of ductility ratio versus tie reinforcement ratio for the tested specimens and analytical specimens in this study. It can be seen that for tie reinforcement ratio, ρ_s = 0.5% which corresponds to approximately 60% of the minimum amount required by the AASHTO [2] seismic provision

Table 4. Analytical results .

Type	R_y (kN)	Δ_y (mm)	R_{max} (kN)	Δ_u (mm)	Ductility ratio Δ_u/Δ_y
H1	125.57	11.9	151.46	56	4.71
H0	123.21	9.38	126.11	73.5	7.84
M1	125.70	11.9	152.22	42.98	3.61
M0	122.71	9.38	126.11	55.3	5.90
L1	126.26	11.9	153.17	31.36	2.64
L0	122.51	9.38	126.79	39.62	4.22

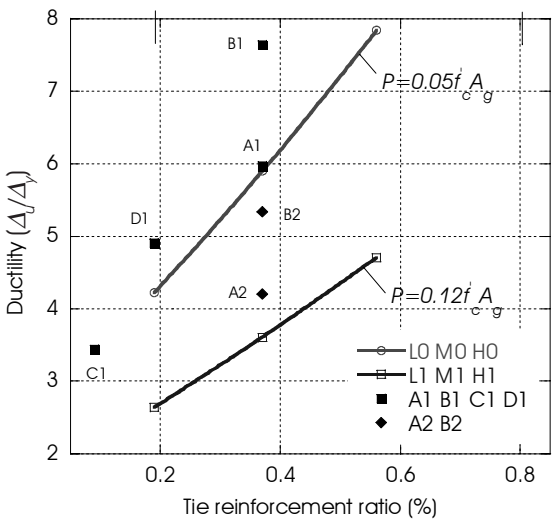

Fig 16. Effect of tie reinforcement on ductility ratio.

(see Eq. 1) the ductility ratios are 4.3 and 7.3 for axial loads of $0.12f'_cA_g$ and $0.05f'_cA_g$ respectively.

Conclusion

The behavior of six bridge pier column models with different amount and arrangement of tie bars subjected to constant axial load and cyclic lateral load was studied experimentally. The cyclic loading tests and verification by fiber element analysis were conducted. It can be found that increasing the amount of tie bars does not affect the maximum lateral load force and the yield lateral force. Increasing the amount of tie bars increases the maximum deflection and ductility ratios of the specimens. The criterion of limiting lateral strain in inner core gave satisfactory estimate of the column deflection. Further analytical study of six specimens with the tie reinforcement ratios varying in the range of 0.19% to 0.56% and subjected to varying cyclic loads was conducted.

Based on the experimental and analytical studies[8], tie reinforcement of the amount required by the AASHTO non-seismic provision at ρ_s = 0.19%, the ductility ratios were 2.8 and 4 for axial load $0.12f'_cA_g$ and $0.05f'_cA_g$ respectively. Tie reinforcement ratio at 0.5% which corresponds to approximately 60% of the minimum amount required by the AASHTO seismic provision, exhibits moderate ductility ratio being 4.3 and 7.3 for axial load $0.12f'_cA_g$ and $0.05f'_cA_g$ respectively.

Acknowledgements

The authors express their sincere appreciation to Professor Kazuhiko Kawashima, for his advice and supports for experimental facility and to Gakuho Watanabe for constructing and supervision during the tests. Financial support for this research provided by The Thailand Research Fund is gratefully acknowledged.

References

1 Warnitchai, P. and Lisantono, A. (1996) Probabilistic Seismic Risk Mapping for Thailand, *Proc. of the Eleventh Conference on Earthquake Engineering, Acapulco, Mexico* 23-8.

2 American Association of State Highway and Transportation Officials, Standard Specifications for Highway Bridge (1992), 15th Edition, Washington, D.C.

3 Wehbe, N.I.,Saiid, M., and Sanders, D. H. (1999) Seismic Performance of Rectangular Bridge Columns with Moderate confinement *ACI Structural Journal*, no. 96-S2

4 Priestley, N. M. J., Seible, F. and Calvi, C.M. (1996) Seismic Design and Retrofit of Bridges John Wiley & Sons.

5 Hoshikuma, J., Kawashima, K., Nagaya, K. and Taylor, A. W. (1997) Stress-Strain Model for Confined Reinforced Concrete in Bridge Piers, *Journal of Structural Engineering, ASCE*, 123(5), 624-33

6 Sakai, J. and Kawashima, K. (2000) An Unloading and Reloading Stress-Strain Model for Concrete Confined by Tie Reinforcements, *Proc. 12th World Conference on Earthquake* Engineering, Auckland, New Zealand, CD-ROM No. 1432

7 Menegotto, M. and Pinto, P.E. (1973) Method of Analysis for Cyclically Loaded R.C. Plane Frames including Changes in Geometry and Non-Elastic Behavior of Elements under Combined Normal Force and Bending, *Proc. of IABSE Symposium on Resistance and Ultimate Deformability of Structures Acted on by Well Defined Repeated Loads*, 15-22

8 Ongsupankul S. (2006) Effectiveness of confining reinforcement on strength and ductility of reinforced concrete highway bridge piers, D. Eng. Thesis, Kasetsart University.